

## Comparative Computational Analysis of Lid Conformation Effects on PET Binding in Fungal Cutinases

Leong Chi Kei<sup>a</sup>, Mohd Shahir Shamsir<sup>a\*</sup>

<sup>a</sup>Department of Bioscience, Faculty of Science, Universiti Teknologi Malaysia, 81310 UTM Skudai, Johor, Malaysia

\*Corresponding author: [shahir@utm.my](mailto:shahir@utm.my)

### Abstract

The enzymatic degradation of Polyethylene Terephthalate (PET) represents a promising sustainable approach to plastic waste management, with fungal cutinases emerging as particularly effective biocatalysts due to their ability to hydrolyse ester linkages in PET polymers. Among the structural factors that may influence catalytic performance, lid conformation appears to play a critical role in substrate accessibility and binding efficiency. Fungal cutinases exhibit diverse conformational states, ranging from open-lid structures that provide direct substrate access to closed-lid conformations that may regulate catalytic activity through controlled substrate binding. This computational study investigates how lid conformation affects PET substrate interactions by comparing two structurally distinct fungal cutinases: *FoCut5a* from *Fusarium oxysporum*, which exhibits an open-lid conformation, and *Tr* cutinase from *Trichoderma reesei*, characterized by a closed-lid structure. Through integrated sequence alignment, structural analysis, and molecular docking approaches, we examined the relationship between conformational state and PET binding capability. Sequence analysis revealed 39.1% similarity between the enzymes, with both containing the essential Ser-His-Asp catalytic triad and the GYSQG motif characteristic of fungal PET-degrading cutinases. While structural superimposition confirmed conserved active site architecture, the enzymes displayed markedly different substrate accessibility profiles. Molecular docking analysis demonstrated comparable binding affinities among all tested cutinases (*Fsp* cutinase: -5.27 kcal/mol, *FoCut5a*: -5.113 kcal/mol, *Tr* cutinase: -5.068 kcal/mol). However, significant differences emerged in substrate binding orientation: open-lid conformations facilitated proper positioning of PET ligands at catalytic serine residues, whereas the closed-lid structure resulted in alternative binding modes to non-catalytic sites. Additionally, a flexible hinge region was identified in *Tr* cutinase that may regulate lid dynamics and substrate access. These findings suggest that lid conformation represents a key structural determinant of substrate accessibility in fungal cutinases, though experimental validation is necessary to confirm the biological significance of these computational predictions. The structural insights gained provide a foundation for rational enzyme design strategies aimed at optimizing PET degradation capabilities through targeted modifications of lid architecture and dynamics.

**Keywords:** cutinase; PET; open-lid; closed-lid; bioinformatics tools

### Introduction

Plastic is a type of synthetic polymer which is man-made from monomers derived from oil or gas through the process of polymerization. Although plastic can be broken down, it is not biodegradable. It can take up to hundreds or thousands of years to degrade (Berry et al., 2023). With the evolution of industrial advancement starting in the 1940s, the plastics industry was unlocked by the manufacturing technologies of the materials. According to the World Bank Group report, plastic comprises about 5 to 12% of the total waste generated worldwide, with 20 to 30% by weight. Approximately 60% of plastics enter the environment as plastic waste. The plastic waste generated had reached more than 360 million

tonnes (MT) in 2018 from 0.35 MT annual production in 1950, with an 8.4% annual growth rate (Kibria et al., 2023).

Polyethylene terephthalate (PET) is a thermoplastic polymer categorized in the polyester family due to the ester functionalities within its molecules. In recent years, the demand for using PET has continuously increased and has become the third most commonly used plastic in the packaging industry (Nisticò, 2020). PET waste can be disposed of in various ways, including landfills, incineration through thermal treatment, recycling, and biodegradation. Considering PET is extremely durable and may release hazardous chemicals when burning or reacting, biodegradation is the method of choice that is prioritized in the current day (Koshti et al., 2018). The enzymatic degradation is the main focus of current research because PET is composed of monomers linked by ester linkages, which can be hydrolyzed by hydrolytic enzymes such as cutinase, lipase, and PETase, which can be obtained from natural sources (Soong et al., 2022).

In addition to microbes, fungi produce cutinase and lipase, the hydrolytic enzymes that are efficient in PET degradation because they can hydrolyze the ester bonds within the monomers. Cutinase is an enzyme expressed by fungal plant pathogens when the pathogens enter the cutin. It breaks down to form the cuticle as a protective layer for the plant. Not only for PET degradation, but cutinase can also be applied in other industries. In the textile industry, cutinase can act as the catalyst in the washing of cotton fibres. The cotton that uses cutinase to wash can remove the cuticle on the cotton, resulting in better wettability (Martínez & Maicas, 2021).

In this research, fungal cutinases are the focus of work. The fungal cutinase from *Fusarium oxysporum* (FoCut5a) and *Trichoderma reesei* (Tr cutinase) are chosen to study due to limited studies. Sequence analysis, structural analysis, and molecular docking were performed on the chosen enzymes to gain a better understanding of PET degradation.

## Materials and methods

To better understand how structural features influence PET degradation efficiency, this study employed a structured computational workflow to compare the PET-degrading capabilities of two fungal cutinases: FoCut5a from *Fusarium oxysporum* (UniProt Access Number: X0BTD8, PDB ID: 5AJH) and Tr cutinase from *Trichoderma reesei* (UniProt Access Number: A0A024SC78, PDB ID: 4PSC). The research design integrated both sequence alignment and structural analysis to elucidate the similarities and differences between FoCut5a and Tr cutinase, with a particular focus on active accessibility, lid conformation, and protein-ligand interaction through molecular docking.

The analysis began with the first part, enzyme analysis. The amino acid sequences of FoCut5a and Tr cutinase in FASTA format were retrieved from UniProt and underwent a pairwise sequence alignment in EMBL-EBI. To identify the conserved motif shared between FoCut5a and Tr cutinase, a multiple sequence alignment was done on FoCut5a, Tr cutinase and other bacterial or fungal enzymes, providing the same ability to degrade PET. Moreover, the amino acid composition of FoCut5a and Tr cutinase were calculated in ProtParam and classified the amino acids based on the category. To gain a better understanding of FoCut5a and Tr cutinase, a secondary structure analysis was performed. The secondary structure analysis involved determining the percentage composition of secondary structure elements using the SOPMA tool, based on the enzyme sequences in FASTA format. Additionally, the 3D models of FoCut5a and Tr cutinase were evaluated using a Ramachandran plot generated by PROCHECK to assess the stereochemical quality and evaluate the distribution of dihedral angles or any conformational outliers. The structural superimposition and active sites identification were performed using PyMOL. For the last section, the hinge identification was done only on the closed-lid Tr cutinase.

The second part of this study focused on analyzing protein–ligand interactions between PET and three fungal cutinases, which are Fsp cutinase (PDB ID: 1CEX, control), FoCut5a (PDB ID: 5AJH) and Tr cutinase (PDB ID: 4PSC). The PET ligand structure was retrieved from PubChem (ID: 18721140) and converted to PDB format in Open Babel GUI. Three protein structures were obtained from PDB and prepared in DS Visualizer and AutoDock Tools, respectively. All the PDB formats were saved in PDBQT format, including the PET ligand and the three enzymes. The molecular docking was performed

in AutoDock Vina with the grid box set to cover each active site of the enzyme. Nine docking modes were generated for each complex, and binding affinities were recorded. The best-ranked mode (Mode 1) for each enzyme was visualized using PyMOL and AutoDock Vina viewer to assess ligand orientation, hydrogen bonding, and interaction with the catalytic triad.

## Results and discussion

*FoCut5a* and *Tr* cutinase showed a 39.1% similarity based on the pairwise sequence alignment, indicating moderate evolutionary relatedness. While the sequence identity was 26.2%, this level of similarity suggests potential homology between the enzymes. A conserved region motif with GYSQG was identified and shared between *FoCut5a* and *Tr* cutinase (Figure 1).

X08TD8_FUSOX	1	-----MKFSIISTL	9
CUTI1_HYPJR	1	MRSAILTTLLAGHAFYKPAQSVNRDWPISINEFLSELAKVMPIGDT	50
X08TD8_FUSOX	10	LAATASALPAGQDAALAEARQLGGSITRNDLANGSGSCPGVIFIYARGS	59
CUTI1_HYPJR	51	ITAACDLISDGEDAA--ASLFGISETEND-----PCGDVTVLFARGT	90
X08TD8_FUSOX	60	TESGNLGLT-LGPRVASKLEAKYGKNGVWIQGVGGAYRATLGD---NALPR	105
CUTI1_HYPJR	91	CDPGNVGVLVGPWFDSLTALGSRTLGVKGV--PYPASVQDFLSGGSVQN	138
X08TD8_FUSOX	106	GTSSA-AIREMLGHFSDANQKCPDAVLIAQGYSQGRALAAASVTDVDAGI	154
CUTI1_HYPJR	139	GINMANQIKSVL-----QSCPNTKLVLGYSQGMVVHNAASNLDAAT	181
X08TD8_FUSOX	155	REKIAGVVLFG--YTKNLQNRGKIPSYEDRTKVCNTGDLVCTGSLIV	201
CUTI1_HYPJR	182	MSKISAVLVFGDPYGGKPVAN-----FDAAKTLVCHDGDNICQGGDII	225
X08TD8_FUSOX	202	AAPHLAYQSAASGAPEFLIQKADAAGAA	230
CUTI1_HYPJR	226	LLPHLYAEDADTAA-AFVVPLVS-----	248

**Figure 1** Pairwise sequence alignment of *FoCut5a* with PDB ID: 5AJH and *Tr* cutinase with PDB ID: 4PSC generated using EMBL-EBI. The orange box indicates a conserved motif shared between *FoCut5a* and *Tr* cutinase.

To better understand the functional significance of the conserved motif, multiple sequence alignment was performed on 19 enzymes, including two bacterial and 15 fungal enzymes with known PET-degrading capabilities. The analysis revealed the characteristic GX SXG motif commonly found in PET-degrading enzymes, where the variable positions show taxonomic specificity: fungal enzymes typically display GYSQG while bacterial enzymes show GWSMG or GHSMG variants (Figure 2). This motif is crucial for ester bond hydrolysis in PET polymers (H. Zhang et al., 2023). The presence of the GYSQG motif in both *FoCut5a* and *Tr* cutinase confirms their classification as fungal PET-degrading enzymes.

sp|A0A0K8P6T7|PETH\_PISS1 MNFPRASRLMQAAVLGGLMAVSAAT 26  
 tr|H4WVX38|H4WVX3\_9ACTN 0  
 tr|A0A395NU92|A0A395NU92\_TRIAR 58  
 tr|G0MGS4|G0MGS4\_HYPVG 58  
 tr|A0A0F9X9J3|A0A0F9X9J3\_TRIHA 57  
 tr|A0A0AE1HL3|A0A0AE1HL3\_9HYPO 57  
 tr|A0A024BIB3|A0A024BIB3\_9HYPO 57  
 sp|A0A0245C78|CUT11\_HYPIR 57  
 sp|G0R8H3|CUT11\_HYPIQ 57  
 tr|A0A024CAW6|A0A024CAW6\_TRILO 57  
 sp|P2956|CUT11\_ASPOR 26  
 tr|X0BTD8|X0BTD8\_FUSOX 31  
 tr|A0A084HLCY4|A0A084HLCY4\_FUSOX 31  
 tr|A0A0C4D37|A0A0C4D37\_FUSOF 31  
 tr|A0A0J9W9K4|A0A0J9W9K4\_FUSO4 31  
 tr|A0A02H3TNX8|A0A02H3TNX8\_FUSOX 31  
 tr|A0A02H3GLG6|A0A02H3GLG6\_FUSOX 31  
 sp|Q99174|CUT1\_FUSC 31  
 sp|P00590|CUT11\_FUSVN 31

## A0A0K8P6T7:Signal

sp|A0A0K8P6T7|PETH\_PISS1 AQTNPYARGPNPTAASLEASAGPFTVRSFTVSR--PSGYAGT 67  
 tr|H4WVX38|H4WVX3\_9ACTN 42  
 tr|A0A395NU92|A0A395NU92\_TRIAR 117  
 tr|G0MGS4|G0MGS4\_HYPVG 116  
 tr|A0A0F9X9J3|A0A0F9X9J3\_TRIHA 116  
 tr|A0A0AE1HL3|A0A0AE1HL3\_9HYPO 116  
 tr|A0A024BIB3|A0A024BIB3\_9HYPO 116  
 sp|A0A0245C78|CUT11\_HYPIR 116  
 sp|G0R8H3|CUT11\_HYPIQ 116  
 tr|A0A024CAW6|A0A024CAW6\_TRILO 116  
 sp|P2956|CUT11\_ASPOR 73  
 tr|X0BTD8|X0BTD8\_FUSOX 84  
 tr|A0A084HLCY4|A0A084HLCY4\_FUSOX 84  
 tr|A0A0C4D37|A0A0C4D37\_FUSOF 84  
 tr|A0A0J9W9K4|A0A0J9W9K4\_FUSO4 84  
 tr|A0A02H3TNX8|A0A02H3TNX8\_FUSOX 84  
 tr|A0A02H3GLG6|A0A02H3GLG6\_FUSOX 84  
 sp|Q99174|CUT1\_FUSC 83  
 sp|P00590|CUT11\_FUSVN 83

## A0A0K8P6T7:Signal

sp|A0A0K8P6T7|PETH\_PISS1 VYPTNAGTVGAIAIPVGYTARQSSI KWWGPRLASHGFVVITIDTNSTLDQPPSSRSQMAALRQ 137  
 tr|H4WVX38|H4WVX3\_9ACTN 103  
 tr|A0A395NU92|A0A395NU92\_TRIAR 142  
 tr|G0MGS4|G0MGS4\_HYPVG 141  
 tr|A0A0F9X9J3|A0A0F9X9J3\_TRIHA 141  
 tr|A0A0AE1HL3|A0A0AE1HL3\_9HYPO 141  
 tr|A0A024BIB3|A0A024BIB3\_9HYPO 141  
 sp|A0A0245C78|CUT11\_HYPIR 141  
 sp|G0R8H3|CUT11\_HYPIQ 141  
 tr|A0A024CAW6|A0A024CAW6\_TRILO 141  
 sp|P2956|CUT11\_ASPOR 103  
 tr|X0BTD8|X0BTD8\_FUSOX 114  
 tr|A0A084HLCY4|A0A084HLCY4\_FUSOX 114  
 tr|A0A0C4D37|A0A0C4D37\_FUSOF 114  
 tr|A0A0J9W9K4|A0A0J9W9K4\_FUSO4 114  
 tr|A0A02H3TNX8|A0A02H3TNX8\_FUSOX 114  
 tr|A0A02H3GLG6|A0A02H3GLG6\_FUSOX 114  
 sp|Q99174|CUT1\_FUSC 113  
 sp|P00590|CUT11\_FUSVN 113

## A0A0K8P6T7:Signal

sp|A0A0K8P6T7|PETH\_PISS1 VASLNGTSSSPIYGVKVDRTARMGVMSWGGGSL-----ISAANNPSLKAAAPQ 182  
 tr|H4WVX38|H4WVX3\_9ACTN 153  
 tr|A0A395NU92|A0A395NU92\_TRIAR 201  
 tr|G0MGS4|G0MGS4\_HYPVG 200  
 tr|A0A0F9X9J3|A0A0F9X9J3\_TRIHA 200  
 tr|A0A0AE1HL3|A0A0AE1HL3\_9HYPO 200  
 tr|A0A024BIB3|A0A024BIB3\_9HYPO 200  
 sp|A0A0245C78|CUT11\_HYPIR 200  
 sp|G0R8H3|CUT11\_HYPIQ 200  
 tr|A0A024CAW6|A0A024CAW6\_TRILO 200  
 sp|P2956|CUT11\_ASPOR 165  
 tr|X0BTD8|X0BTD8\_FUSOX 176  
 tr|A0A084HLCY4|A0A084HLCY4\_FUSOX 176  
 tr|A0A0C4D37|A0A0C4D37\_FUSOF 176  
 tr|A0A0J9W9K4|A0A0J9W9K4\_FUSO4 176  
 tr|A0A02H3TNX8|A0A02H3TNX8\_FUSOX 176  
 tr|A0A02H3GLG6|A0A02H3GLG6\_FUSOX 176  
 sp|Q99174|CUT1\_FUSC 173  
 sp|P00590|CUT11\_FUSVN 173

## A0A0K8P6T7:Signal

sp|A0A0K8P6T7|PETH\_PISS1 APWDSSTNFSS-----VTVPTLIFACENDSIAPVNSSALPIYDSMSRN-AKQFLEING 234  
 tr|H4WVX38|H4WVX3\_9ACTN 206  
 tr|A0A395NU92|A0A395NU92\_TRIAR 239  
 tr|G0MGS4|G0MGS4\_HYPVG 238  
 tr|A0A0F9X9J3|A0A0F9X9J3\_TRIHA 238  
 tr|A0A0AE1HL3|A0A0AE1HL3\_9HYPO 238  
 tr|A0A024BIB3|A0A024BIB3\_9HYPO 238  
 sp|A0A0245C78|CUT11\_HYPIR 238  
 sp|G0R8H3|CUT11\_HYPIQ 238  
 tr|A0A024CAW6|A0A024CAW6\_TRILO 238  
 sp|P2956|CUT11\_ASPOR 202  
 tr|X0BTD8|X0BTD8\_FUSOX 214  
 tr|A0A084HLCY4|A0A084HLCY4\_FUSOX 214  
 tr|A0A0C4D37|A0A0C4D37\_FUSOF 214  
 tr|A0A0J9W9K4|A0A0J9W9K4\_FUSO4 214  
 tr|A0A02H3TNX8|A0A02H3TNX8\_FUSOX 214  
 tr|A0A02H3GLG6|A0A02H3GLG6\_FUSOX 214  
 sp|Q99174|CUT1\_FUSC 213  
 sp|P00590|CUT11\_FUSVN 213

## A0A0K8P6T7:Signal

sp|A0A0K8P6T7|PETH\_PISS1 GSHSCANSNGSNQALIGKKGVAMMKRFMDNDTRYSTACENPNSTRVSDFRITAN--CS- 290  
 tr|H4WVX38|H4WVX3\_9ACTN 262  
 tr|A0A395NU92|A0A395NU92\_TRIAR 248  
 tr|G0MGS4|G0MGS4\_HYPVG 248  
 tr|A0A0F9X9J3|A0A0F9X9J3\_TRIHA 248  
 tr|A0A0AE1HL3|A0A0AE1HL3\_9HYPO 248  
 tr|A0A024BIB3|A0A024BIB3\_9HYPO 248  
 sp|A0A0245C78|CUT11\_HYPIR 248  
 sp|G0R8H3|CUT11\_HYPIQ 248  
 tr|A0A024CAW6|A0A024CAW6\_TRILO 248  
 sp|P2956|CUT11\_ASPOR 213  
 tr|X0BTD8|X0BTD8\_FUSOX 230  
 tr|A0A084HLCY4|A0A084HLCY4\_FUSOX 230  
 tr|A0A0C4D37|A0A0C4D37\_FUSOF 230  
 tr|A0A0J9W9K4|A0A0J9W9K4\_FUSO4 230  
 tr|A0A02H3TNX8|A0A02H3TNX8\_FUSOX 230  
 tr|A0A02H3GLG6|A0A02H3GLG6\_FUSOX 230  
 sp|Q99174|CUT1\_FUSC 230  
 sp|P00590|CUT11\_FUSVN 230

## A0A0K8P6T7:Signal

sp|A0A0K8P6T7|PETH\_PISS1 GSHSCANSNGSNQALIGKKGVAMMKRFMDNDTRYSTACENPNSTRVSDFRITAN--CS- 290  
 tr|H4WVX38|H4WVX3\_9ACTN 262  
 tr|A0A395NU92|A0A395NU92\_TRIAR 248  
 tr|G0MGS4|G0MGS4\_HYPVG 248  
 tr|A0A0F9X9J3|A0A0F9X9J3\_TRIHA 248  
 tr|A0A0AE1HL3|A0A0AE1HL3\_9HYPO 248  
 tr|A0A024BIB3|A0A024BIB3\_9HYPO 248  
 sp|A0A0245C78|CUT11\_HYPIR 248  
 sp|G0R8H3|CUT11\_HYPIQ 248  
 tr|A0A024CAW6|A0A024CAW6\_TRILO 248  
 sp|P2956|CUT11\_ASPOR 213  
 tr|X0BTD8|X0BTD8\_FUSOX 230  
 tr|A0A084HLCY4|A0A084HLCY4\_FUSOX 230  
 tr|A0A0C4D37|A0A0C4D37\_FUSOF 230  
 tr|A0A0J9W9K4|A0A0J9W9K4\_FUSO4 230  
 tr|A0A02H3TNX8|A0A02H3TNX8\_FUSOX 230  
 tr|A0A02H3GLG6|A0A02H3GLG6\_FUSOX 230  
 sp|Q99174|CUT1\_FUSC 230  
 sp|P00590|CUT11\_FUSVN 230



**Figure 2** Multiple Sequence Alignment of *FoCut5a*, *Tr* cutinase and other bacterial or fungal enzymes performed using UniProt. Ticked boxes indicate *Tr* cutinase and *FoCut5a*, conserved regions are highlighted in purple and red circles the conserved motif shared among the enzymes.

The catalytic triad (Ser-His-Asp) functions to catalyze the hydrolysis of ester bonds that link PET polymers in PET plastic (Liang & Zou, 2022). *FoCut5a* and *Tr* cutinase both have the catalytic triad but are located at different locations in the amino acid sequences. In the superimposition between *FoCut5a* and *Tr* cutinase, three of the active sites for each enzyme overlapped and were aligned together (Figure 3). The same alignment of the active sites indicates that they have similar catalytic reactions. The proximity of the amino acids in the active site for *FoCut5a* and *Tr* cutinase was due to the precise three-dimensional alignment of the amino acid sequences. The structural flexibility of the active site offers high catalytic efficiency to *FoCut5a* and *Tr* cutinase, which may help improve their binding affinity with the PET ligand (Saikia & Ramakrishnan, 2022). In the view of surface representation, the aspartate active site of *FoCut5a* was exposed on the surface, as the hydrophobic lid did not cover it, allowing the PET substrate to interact easily. The lid of *Tr* cutinase was seen at the outside, but all the active sites were covered (Figure 4).

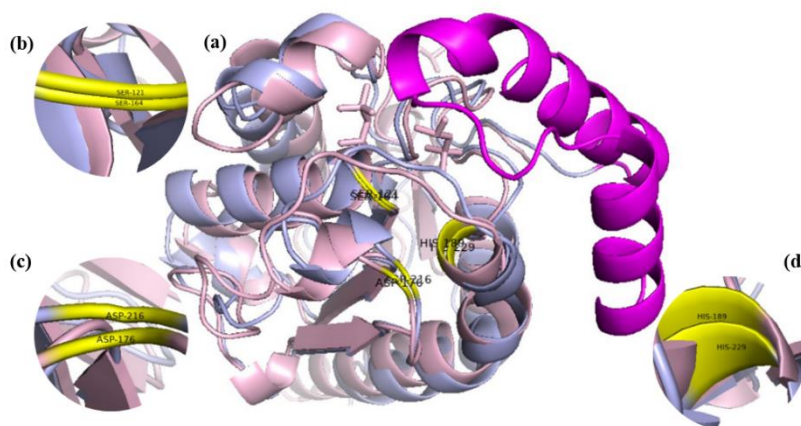


**Figure 3** Superimposition of *FoCut5a* and *Tr* cutinase: (a) ribbon Representation of *FoCut5a* (pink) and *Tr* cutinase (purple), (b) serine active site, (c) aspartate active site and (d) histidine active site.

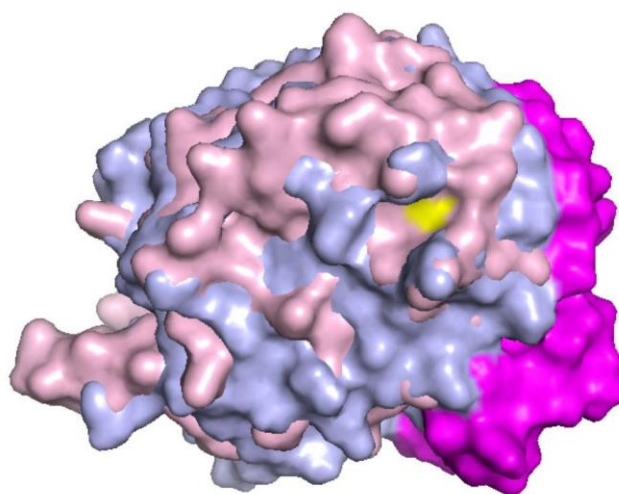


**Figure 4** Surface representation of *FoCut5a* (pink) and *Tr* cutinase (purple) with only the aspartate active site from *FoCut5a* shown.

**Table 1:** Amino Acid Content in *FoCut5a* and *Tr* cutinase calculated using ProtParam

Fungal Cutinases		<i>FoCut5a</i>		<i>Tr</i> cutinase	
Amino Acid Group	Number	Percentage (%)	Number	Percentage (%)	
<b>(A) Flexible</b>					
<b>Alanine (A) Ala</b>	<b>40</b>	<b>17.4</b>	<b>28</b>	<b>11.3</b>	
Serine (S) Ser	18	7.8	20	8.1	
Threonine (T) Thr	12	5.2	14	5.6	
Glycine (G) Gly	29	12.6	22	8.9	
Proline (P) Pro	9	3.9	15	6.0	
Total	<b>108</b>	<b>46.9</b>	<b>99</b>	<b>39.9</b>	
<b>(B) Charged</b>					
Lysine (K) Lys	10	4.3	8	3.2	
Arginine (R) Arg	10	4.3	5	2.0	
Histidine (H) His	2	0.9	4	1.6	
Aspartate (D) Asp	10	4.3	18	7.3	
Glutamate (E) Glu	7	3.0	6	2.4	
Total	39	16.8	41	16.5	
<b>(C) Aromatic</b>					
Phenylalanine (F) Phe	6	2.6	10	4.0	
Tryptophan (W) Trp	1	0.4	2	0.8	
Tyrosine (Y) Tyr	7	3.0	6	2.4	
Total	14	6.0	18	7.2	
<b>(D) Aliphatic</b>					
Cysteine (C) Cys	4	1.7	6	2.4	
<b>Valine (V) Val</b>	<b>12</b>	<b>5.2</b>	<b>23</b>	<b>9.3</b>	
Leucine (L) Leu	20	8.7	24	9.7	
Isoleucine (I) Ile	13	5.7	12	4.8	
Methionine (M) Met	2	0.9	5	2.0	
Total	<b>51</b>	<b>22.2</b>	<b>70</b>	<b>28.2</b>	
<b>(E) Unclassification</b>					
Asparagine (N) Asn	10	4.3	12	4.8	
Glutamine (Q) Gln	8	3.5	8	3.2	
Total	18	7.8	20	8.0	

*FoCut5a* has a total of 230 amino acids, while *Tr* cutinase has a bigger size with 248 amino acids. Asparagine (N) and glutamine (Q) amino acids were not coloured as they are classified as polar but uncharged residues due to their side chains. The obvious difference between *FoCut5a* and *Tr* cutinase can be seen from the number of amino acids (Table 1). *FoCut5a* had a higher percentage of flexible group, while a higher percentage of aliphatic group was found in *Tr* cutinase. Zooming into the numerical difference of amino acid composition, alanine and valine had a marked difference in the number. *FoCut5a* had 40 alanine, while *Tr* cutinase had only 28 alanine. In contrast, *Tr* cutinase had 23 valines while *FoCut5a* had only 12 valines. Alanine enhances the solubility of protein and the hydrophobic interactions, even though it is small and non-polar. It is crucial in protein-ligand interactions, where it provides flexible regions for both the protein and ligand (Flores-Castañón et al., 2022). For valine, it is a branched, nonpolar side chain which has a strong hydrophobic ability. It is more rigid compared to smaller residues due to the presence of the bulky side chain. Thus, valine enhances the solubility of proteins and the stability of the hydrophobic protein core during protein-ligand interactions (Reifenberg & Zimmer, 2024). Therefore, the presence of alanine in *FoCut5a* allowed it to be more flexible, while the presence of valine in *Tr* cutinase provided the rigidity, which may hinder the PET ligand from interacting with the active sites. Analysis of amino acid composition revealed notable differences between the enzymes (Table 1). *FoCut5a* contains a higher proportion of flexible residues (17.4% vs 11.3%), while *Tr* cutinase has more aliphatic residues (28.2% vs 22.2%). The higher alanine content in *FoCut5a* (40 vs 28 residues) may contribute to increased structural flexibility, while the greater valine content in *Tr* cutinase (23 vs 12 residues) could enhance structural rigidity. However, the direct

correlation between these compositional differences and PET degradation efficiency requires experimental validation and should be interpreted cautiously.

**Table 2:** Summary of Secondary Structure Composition of *FoCut5a* and *Tr* cutinase generated from SOPMA

Secondary Structure	<i>FoCut5a</i>	<i>Tr</i> cutinase
Alpha helix (Hh)	27.43%	<b>31.89%</b>
Extended strand (Ee)	14.16%	13.78 %
Beta turn (Tt)	4.87%	3.54 %
Random coil (Cc)	<b>53.54%</b>	50.79 %

The secondary structure composition of *FoCut5a* and *Tr* cutinase is shown differently in the percentage (Table 2). A higher percentage of alpha helix was found in *Tr* cutinase, at 31.89%, which can provide stability for *Tr* cutinase to withstand higher temperatures (Flores-Castañón et al., 2022). *FoCut5a* had a higher percentage of random coil, which can accommodate substrate molecules over a wider range by providing flexibility to *FoCut5a* during conformational changes (Kumar et al., 2024). Ramachandran plot analysis showed that 91.8% of residues in *FoCut5a* and 94.6% in *Tr* cutinase were located in the most favoured regions, indicating good stereochemical quality and overall structural reliability for both enzyme models (Figure 5). Over 90% of the residues were in the most favoured regions, indicating that the models of *FoCut5a* and *Tr* cutinase were accurate and valid for use in the research (Goswami et al., 2024).

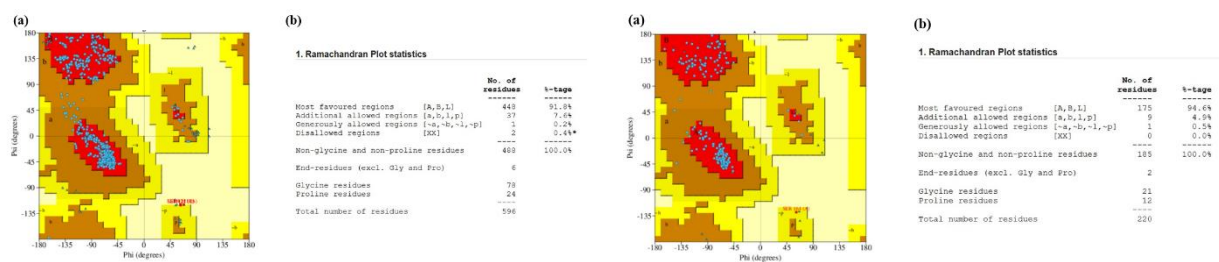


**Figure 5** Ramachandran Plot of *FoCut5a* (left) and *Tr* cutinase (right) generated from PROCHECK

*Tr* cutinase contains a lid that blocks substrate access to the active site, and its movement is regulated by a hinge, which is a short, flexible amino acid sequence acting as a pivot. Using PACKMAN-Molecule, a hinge region from residues 72 to 77 was identified, which is located near the lid and composed of serine, glutamine, asparagine, threonine and aspartate (Figure 6). Although only Hinge 1 had a p-value above 0.05 (0.128), it was accepted due to its proximity to the lid.

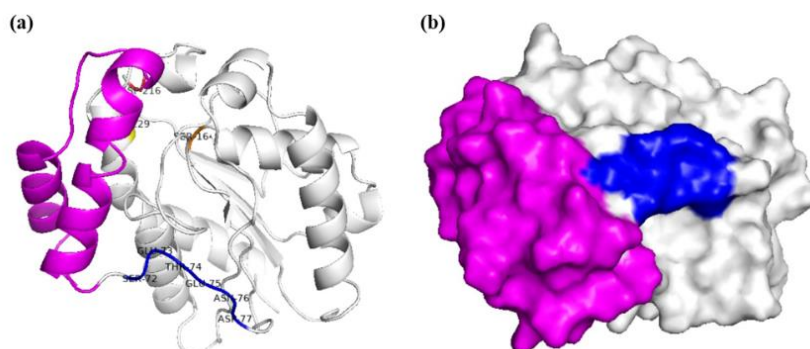


**Figure 6** Representation of the lid (magenta) and hinge (blue) of *Tr* cutinase in PyMOL: (a) ribbon representation and (b) surface representation.

**Table 3:** Summary of Docking results from AutoDock Vina

	<i>Fsp</i> cutinase	<i>FoCut5a</i>	<i>Tr</i> cutinase
Best binding affinity (kcal/mol)	-5.27	-5.113	-5.068
Bind to active site	Yes (Ser 120)	Yes (Ser 121)	No (Asp 237)

Molecular docking analysis revealed similar binding affinities among all three enzymes: *Fsp* cutinase (-5.27 kcal/mol), *FoCut5a* (-5.113 kcal/mol) and *Tr* cutinase (-5.068 kcal/mol) (Table 3). Importantly, the differences between these values are small (within 0.2 kcal/mol) and fall within the typical uncertainty range of computational docking predictions, suggesting that all three enzymes may have comparable binding potential for PET substrates.

However, a critical difference emerged in the binding mode analysis. Both *Fsp* cutinase and *FoCut5a* successfully positioned the PET ligand at their catalytic serine residues (Ser120 and Ser121, respectively), indicating proper orientation for catalytic attack. In contrast, the PET ligand bound to Asp237 in *Tr* cutinase rather than the catalytic serine (Figure 7). This deviation likely reflects the steric hindrance imposed by the closed-lid conformation observed in the crystal structure.

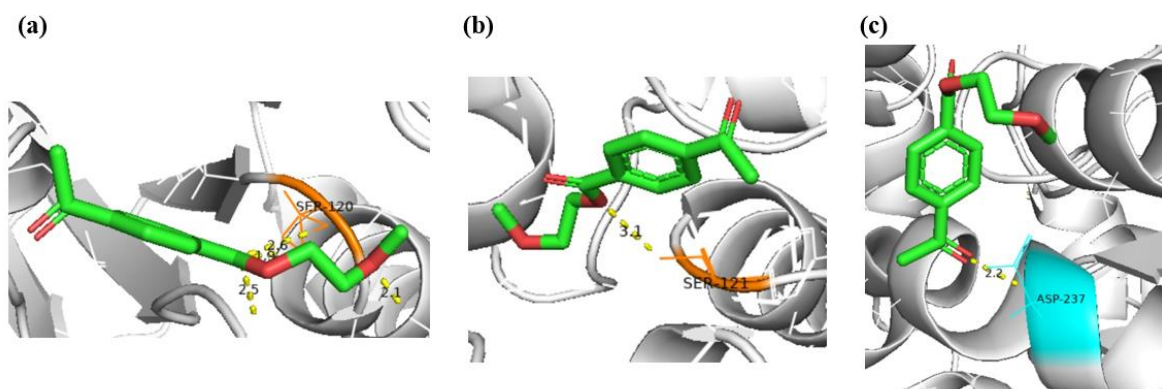


**Figure 7** Binding interactions of PET ligand with (a) *Fsp* cutinase (Ser120), (b) *FoCut5a* (Ser121) and (c) *Tr* cutinase (Asp237). PET was correctly positioned at the catalytic serine in *Fsp* cutinase and *FoCut5a*, while in *Tr* cutinase, the ligand interacted incorrectly with Asp237, likely due to the closed-lid conformation. Binding distances are shown in Å.

Several important limitations should be considered when interpreting these results. First, the molecular docking employed rigid protein structures, which may not capture the dynamic conformational changes that occur during enzyme-substrate interactions. The closed-lid conformation of *Tr* cutinase observed in the crystal structure may not represent its catalytically active state, as lid opening could occur upon substrate binding through induced-fit mechanisms.

Second, the small molecule PET analogue used in docking may not accurately represent the behaviour of the actual PET polymer, which involves complex surface interactions and multiple binding events during degradation. Real PET degradation is a multi-step process that depends on factors not captured in single-molecule docking studies, including polymer chain accessibility, crystallinity, and surface topology.

Third, the computational predictions require experimental validation to confirm their biological relevance. Factors such as enzyme kinetics, thermal stability, optimal reaction conditions and actual PET degradation rates cannot be accurately predicted from structural analysis alone.

Finally, the binding affinity differences observed are within the margin of error typical for computational docking studies, and their biological significance remains uncertain without experimental confirmation.



## Conclusion

This computational study provides preliminary insights into the structural features that may influence PET degradation capabilities of fungal cutinases. Sequence analysis revealed moderate similarity (39.1%) between *FoCut5a* and *Tr* cutinase, with both enzymes containing the characteristic GYSQG motif that defines fungal PET-degrading cutinases. The presence of conserved catalytic triads and aligned active sites suggests both enzymes possess the fundamental molecular machinery required for ester bond hydrolysis.

The most significant finding relates to the potential impact of lid conformation on substrate accessibility. While all three enzymes (*Fsp* cutinase, *FoCut5a*, and *Tr* cutinase) showed comparable binding affinities to PET in molecular docking analysis (differences within 0.2 kcal/mol), the binding orientations differed substantially. The open-lid conformations of *Fsp* cutinase and *FoCut5a* facilitated proper positioning of the PET ligand at the catalytic serine residues, whereas the closed-lid structure of *Tr* cutinase resulted in alternative binding to a non-catalytic aspartate residue.

However, several important caveats must be considered. The computational approach employed rigid protein structures that may not capture the dynamic conformational changes occurring during enzyme-substrate interactions. The closed-lid conformation observed in *Tr* cutinase's crystal structure may not represent its sole catalytically relevant state, as lid opening could potentially occur through induced-fit mechanisms upon substrate binding. Furthermore, the small PET analogue used in docking studies may not accurately reflect the complex interactions involved in actual polymer degradation, which is a multi-step process dependent on numerous factors including polymer crystallinity, surface accessibility and reaction conditions.

The binding affinity differences observed are small and within the typical uncertainty range of computational docking predictions, making their biological significance unclear without experimental validation. Additionally, the correlations suggested between amino acid composition, secondary structure content and enzymatic performance require empirical confirmation.

## Acknowledgement

This work is part of the Final Year Undergraduate Project for Bachelor of Science (Industrial Biology) with Honours Degree Program conducted by Department of Bioscience, Faculty of Science, Universiti Teknologi Malaysia.

## References

- Berry, K. L. E., Hall, N., Critchell, K., Chan, K., Bennett, B., Mortimer, M., & Lewis, P. J. (2023). Plastics. In *Springer Textbooks in Earth Sciences, Geography and Environment* (pp. 207–228).
- Flores-Castañón, N., Sarkar, S., & Banerjee, A. (2022). Structural, functional, and molecular docking analyses of microbial cutinase enzymes against polyurethane monomers. *Journal of Hazardous Materials Letters*, 3, 100063.
- Goswami, V., Patel, D., Rohit, S., Chaube, U., & Patel, B. (2024). Homology modeling, binding site identification, molecular docking and molecular dynamics simulation study of emerging and promising drug target of Wnt signaling – Human Porcupine enzyme. *Results in Chemistry*, 7, 101482.
- Kibria, M. G., Masuk, N. I., Safayet, R., Nguyen, H. Q., & Mourshed, M. (2023). Plastic waste: Challenges and opportunities to mitigate pollution and effective management. *International Journal of Environmental Research*, 17(1).
- Koshti, R., Mehta, L., & Samarth, N. (2018). Biological recycling of polyethylene terephthalate: A mini-review. *Journal of Polymers and the Environment*, 26(8), 3520–3529.
- Kumar, S., Chaudhary, B., & Singhal, B. (2024). Phylum-level studies of bacterial cutinases for unravelling enzymatic specificity toward PET degradation: An in silico approach. *Brazilian Journal of Microbiology*.
- Liang, X., & Zou, H. (2022). Biotechnological application of cutinase: A powerful tool in synthetic biology. *SynBio*, 1(1), 54–64.

- Martínez, A., & Maicas, S. (2021). Cutinases: Characteristics and insights in industrial production. *Catalysts*, 11(10), 1194.
- Nisticò, R. (2020). Polyethylene terephthalate (PET) in the packaging industry. *Polymer Testing*, 90, 106707.
- Reifenberg, P., & Zimmer, A. (2024). Branched-chain amino acids: Physico-chemical properties, industrial synthesis and role in signaling, metabolism and energy production. *Amino Acids*, 56(1).
- Saikia, J., & Ramakrishnan, V. (2022). Peptide nanocatalysts. In *Elsevier eBooks* (pp. 173–206).
- Soong, Y. V., Sobkowicz, M. J., & Xie, D. (2022). Recent advances in biological recycling of polyethylene terephthalate (PET) plastic wastes. *Bioengineering*, 9(3), 98.
- Zhang, H., Dierkes, R. F., Perez-Garcia, P., Costanzi, E., Dittrich, J., Cea, P. A., Gurschke, M., Applegate, V., Partus, K., Schmeisser, C., Pflieger, C., Gohlke, H., Smits, S. H. J., Chow, J., & Streit, W. R. (2023). The metagenome-derived esterase PET40 is highly promiscuous and hydrolyses polyethylene terephthalate (PET). *FEBS Journal*, 291(1), 70–91.